0026-895X/09/7504-751–761$20.00
MOLECULAR PHARMACOLOGY
Copyright © 2009 The American Society for Pharmacology and Experimental Therapeutics
Mol Pharmacol 75:751–761, 2009

Vol. 75, No. 4
51623/3446694
Printed in U.S.A.

Anterograde Trafficking of G Protein-Coupled Receptors: Function of the C-Terminal $F(X)_6LL$ Motif in Export from the Endoplasmic Reticulum

Matthew T. Duvernay, Chunmin Dong, Xiaoping Zhang, Fuguo Zhou, Charles D. Nichols, and Guangyu Wu

Department of Pharmacology and Experimental Therapeutics, Louisiana State University Health Sciences Center, New Orleans, Louisiana

Received August 28, 2008; accepted December 30, 2008

ABSTRACT

We have reported previously that the $F(X)_6LL$ motif in the C termini is essential for export of α_{2B}-adrenergic (α_{2B}-AR) and angiotensin II type 1 receptors (AT1Rs) from the endoplasmic reticulum (ER). Here, we further demonstrate that mutation of the $F(X)_6LL$ motif similarly abolished the cell-surface expression of α_{2B}-AR, AT1R, α_{1B}-AR, and β_2-AR, suggesting that the $F(X)_6LL$ motif plays a general role in ER export of G protein-coupled receptors (GPCRs). Mutation of Phe to Val, Leu, Trp, and Tyr, and mutation of LL to FF and VV, markedly inhibited α_{2B}-AR transport, indicating that the $F(X)_6LL$ function cannot be fully substituted by other hydrophobic residues. The structural analysis revealed that the Phe residue in the $F(X)_6LL$ motif is buried in the transmembrane domains and possibly interacts with Ile58 in β_2-AR and Val42 in α_{2B}-AR, whereas the LL motif is exposed to the cytosolic space. Indeed, mutation of Ile58 in β_2-AR and Val42 in α_{2B}-AR markedly disrupted cell surface transport of the receptors. It is noteworthy that the Val and Ile residues are highly conserved among the GPCRs carrying the $F(X)_6LL$ motif. Furthermore, the Phe mutant exhibited a stronger interaction with ER chaperones and was more potently rescued by physical and chemical treatments than the LL mutant. These data suggest that the Phe residue is probably involved in folding of α_{2B}-AR and β_2-AR, possibly through interaction with other hydrophobic residues in neighboring domains. These data also provide the first evidence implying crucial roles of the C termini possibly through modulating multiple events in anterograde trafficking of GPCRs.

G protein-coupled receptors (GPCRs) constitute a superfamily of cell-surface receptors that regulate the cellular responses to a broad spectrum of ligands (Pierce et al., 2002). These GPCRs share common structure features characterized by a core of seven transmembrane (TM)-spanning α-helices, three intracellular loops, three extracellular loops, an extracellular N terminus, and an intracellular C terminus (CT). Whereas the transmembrane core, N terminus, and extracellular loops are involved in ligand recognition, the CT and intracellular loops are involved in the regulation of G protein coupling, phosphorylation, and intracellular trafficking (von Zastrow, 2003).

Export from the endoplasmic reticulum (ER) of GPCRs represents the first step in intracellular trafficking of the receptors and influences the cell-surface expression and function of the receptors (Petaja-Repo et al., 2000; Dong et al., 2007). GPCRs are synthesized in the ER. Once correctly assembled and properly folded into their native conformations, the receptors become available for recruitment into ER-derived COPII transport vesicles, which exclusively mediate protein transport from the ER (Dong et al., 2008). It has been well demonstrated that physical interaction of plasma membrane proteins including GPCRs with the ER resident chaperones, such as calnexin and calreticulin, assist the folding and maturation processes to achieve an export-competent

This work was supported by the National Institutes of Health National Institute of General Medical Sciences [Grant R01-GM076167] and National Institutes of Health National Institute of Mental Health [Grant R21-MH078454].

Article, publication date, and citation information can be found at http://molpharm.aspetjournals.org.

doi:10.1124/mol.108.051623.

ABBREVIATIONS: GPCR, G protein-coupled receptor; CT, carboxyl terminus; AT1R, angiotensin II type 1 receptor; AR, adrenergic receptor; ER, endoplasmic reticulum; Ang II, angiotensin II; DMSO, dimethyl sulfoxide; GFP, green fluorescent protein; ERK, extracellular signal-regulated kinase; TM, transmembrane domain; 5-HT, 5-hydroxytryptamine; HEK, human embryonic kidney; DMEM, Dulbecco's modified Eagle's medium; PAGE, polyacrylamide gel electrophoresis; ^{125}I-Ang II, [^{125}I-Sar1, Ile8]angiotensin II; UK14304, 5-bromo-6-(2-imidazolin-2-ylamino)quinoxaline; RX821002, 2-(2,3-dihydro-2-methoxy-1,4-benzodioxin-2-yl)-4,5-dihydro-1H-imidazole; CGP12177, 4-[3-[(1,1-dimethylethyl)amino]-2-hydroxypropoxy]-1,3-dihydro-2*H*-benzimidazol-2-one; [^{3}H]1-NBMeO, *N*-[2-methoxy-^{3}H]-(2-methoxybenzyl)-[2-methoxy-^{3}H]-(2,5-dimethoxy-4-iodophenethylamine; ISO, isoproterenol.

conformation and also prevents export of premature cargo proteins (Morello and Bichet, 2001; Mizrachi and Segaloff, 2004). Recent studies have also shown that export of some proteins from the ER is a selective process and is dictated by specific ER export motifs within the cargo proteins. These ER export motifs mediate the interaction of the cargo proteins with components of the COPII transport machinery to facilitate their recruitment into the COPII vesicles, thereby improving the efficiency of ER export (Nishimura and Balch, 1997; Ma et al., 2001; Wang et al., 2004). The ER-derived vesicles are subsequently targeted to the appropriate downstream compartment. As the initial step in post-translational protein biogenesis, the efficiency of ER export influences the kinetics of receptor maturation. Indeed, ER export has been shown to be the rate-limiting step for the maturation of the G protein-coupled δ-opioid receptor (Petaja-Repo et al., 2000).

It has been well appreciated that the membrane-proximal C-terminal region plays an important role in GPCR export trafficking to the cell surface. The requirement of the C termini for ER export has been demonstrated for a number of GPCRs, including rhodopsin, vasopressin V2, dopamine D1, adenosine A1, α_{2B}-adrenergic (α_{2B}-AR), angiotensin II type 1 (AT1R), and luteinizing hormone/choriogonadotropin receptors (Heymann and Subramaniam, 1997; Pankevych et al., 2003; Duvernay et al., 2004). Mutagenesis studies have identified a number of motifs consisting of hydrophobic residues within the membrane proximal C-terminal region that are required for export from the ER (Schulein et al., 1998; Bermak et al., 2001; Duvernay et al., 2004; Robert et al., 2005). However, the molecular mechanism underlying their function in regulating receptor export remains elusive.

We have demonstrated previously that the $F(X)_6LL$ motif in the membrane-proximal C termini of AT1R and α_{2B}-AR are required for their export from the ER (Duvernay et al., 2004). To define the molecular mechanism underlying the function of the $F(X)_6LL$ motif in mediating GPCR export, we have determined whether these residues are involved in receptor dimerization. We have demonstrated that the mutated α_{2B}-AR, in which the Phe and LL residues in the $F(X)_6LL$ motif were mutated to alanines, forms homodimers and heterodimers with wide-type α_{2B}-AR and functions as a dominant-negative mutant blocking ER export of its wild-type counterpart (Zhou et al., 2006). In this article, we have further characterized the $F(X)_6LL$ motif in GPCRs and elucidated possible molecular mechanisms underlying the function of the $F(X)_6LL$ motif in mediating GPCR export from the ER.

Materials and Methods

Materials. Rat α_{2B}-AR in vector pcDNA3, human β_2-AR in vector pBC, rat AT1R in vector pCDM8 and human α_{1B}-AR tagged with green fluorescent protein (GFP) at its C terminus were kindly provided by Drs. Stephen M. Lanier, Dr. John D. Hildebrandt (Medical University of South Carolina, Charleston, SC), Kenneth E. Bernstein, and Kenneth P. Minneman (Emory University, Atlanta, GA), respectively. Antibodies against GFP, phospho-ERK1/2, calnexin, and calreticulin were purchased from Santa Cruz Biotechnology, Inc. (Santa Cruz, CA). Anti-ERK antibodies detecting total ERK1/2 expression were from Cell Signaling Technology, Inc. (Danvers, MA). The α_2-AR agonist UK14304, rauwolscine, dimethyl sulfoxide (DMSO), and protein G-Sepharose 4B were obtained from Sigma-Aldrich (St. Louis, MO). [^{3}H]RX821002 (specific activity, 41 Ci/mmol), [^{3}H]CGP12177 (51 Ci/mmol), [7-methoxy-^{3}H]prazosin (70 Ci/mmol), and [^{125}I-Sar1, Ile8]angiotensin II (^{125}I-Ang II) (2200 Ci/mmol) were purchased from PerkinElmer Life and Analytical Sciences (Waltham, MA). *N*-[2-Methoxy-^{3}H]-(2-methoxybenzyl)-[2-methoxy-^{3}H]-(2,5-dimethoxy-4-iodophenethylamine ([^{3}H]1-NBMeO), a new radioligand with high affinity for serotonin 2 (5-HT_2) receptors (Braden et al., 2006), was generously provided by the National Institute of Mental Health Chemical Synthesis and Drug Supply Program. The ER marker pDsRed2-ER was from BD Biosciences (San Jose, CA). All other materials were obtained as described elsewhere (Wu et al., 2003; Duvernay et al., 2004; Dong and Wu, 2006).

Plasmid Construction. α_{2B}-AR, β_2-AR, and AT1R tagged with GFP at their C termini were generated as described previously (Wu et al., 2003). A similar strategy was used to tag GFP at the C terminus of 5-HT_{2C} receptor. Our previous studies have shown that the GFP tagging does not influence ligand binding, signaling, and trafficking of the receptors (Duvernay et al., 2004; Dong and Wu, 2006, 2007; Dong et al., 2008). Receptor mutants were generated by using the QuikChange Site-Directed Mutagenesis kit (Stratagene, La Jolla, CA). The sequence of each construct used in this study was verified by restriction mapping and nucleotide sequence analysis (Louisiana State University Health Sciences Center DNA Sequence Core, New Orleans, LA).

Cell Culture and Transient Transfection. HEK293T cells were cultured in Dulbecco's modified Eagle's medium (DMEM) with 10% fetal bovine serum, 100 U/ml penicillin, and 100 U/ml streptomycin. Transient transfection of HEK293T cells was carried out at a cell density of 85 to 90% using Lipofectamine 2000 reagent as described previously (Wu et al., 2003). Transfection efficiency for both six-well and 100-mm dish formats was estimated to be greater than 80% based on the GFP fluorescence.

Intact Cell Ligand Binding. Cell-surface expression of α_{2B}-AR, β_2-AR, AT1R, and α_{1B}-AR in HEK293T cells was measured by ligand binding of intact live cells using [^{3}H]RX821002, [^{3}H]CGP12177, ^{125}I-Ang II, and [7-methoxy-^{3}H]prazosin, respectively, as described previously (Filipeanu et al., 2004, 2006; Dong and Wu, 2006). HEK293T cells cultured on six-well dishes were transiently transfected with 1.0 μg of plasmids. After 6 h, the cells were split into 12-well dishes precoated with poly(L-lysine) at a density of 5×10^5 cells/well. Twenty-four hours after transfection, the cells were serum-starved. Forty-eight hours after transfection, the cells were incubated with DMEM plus [^{3}H]RX821002, [^{3}H]CGP12177, or [7-methoxy-^{3}H]prazosin at a concentration of 20 nM in a total of 400 μl for 90 min at room temperature to measure the cell-surface expression of α_{2B}-AR, β_2-AR, and α_{1B}-AR, respectively. The binding was terminated, and excess radioligand was eliminated by washing the cells twice with ice-cold DMEM. All of the retained radioligand was then extracted by digesting the cells in 1 M NaOH for 2 h at room temperature. The liquid phase was collected and suspended in 5 ml of Ecoscint A scintillation fluid (National Diagnostics Inc., Atlanta, GA). The amount of radioactivity retained was measured by liquid scintillation spectrometry.

For the measurement of AT1R expression at the cell surface, HEK293T cells were incubated with 400 μl of DMEM containing ^{125}I-Ang II at a concentration of 20 pM for 2 h. After washing the cells twice with 1 ml of DMEM, the bound ligand was extracted by mild acid treatment (2×5 min with 0.5 ml of buffer containing 50 mM glycine and 125 mM NaCl, pH 3). The radioactivity was counted in a γ counter. The nonspecific binding of α_{2B}-AR, β_2-AR, α_{1B}-AR, and AT1R was determined in the presence of rauwolscine (10 μM), alprenolol (20 μM), phentolamine (10 μM), and nonradioactive Ang II (10 μM), respectively. All radioligand binding assays were performed in triplicate.

Ligand Binding of Membrane Preparations. HEK293T cells were grown on 15-cm diameter tissue culture plates and transfected with 20 μg of plasmid for wild-type and mutated receptors for 48 h. Membrane preparations and ligand binding of α_{2B}-AR were performed as described previously (Duvernay et al., 2004). For radioligand binding of 5-HT_{2C} receptor, total membrane protein was incu-

bated with [^{3}H]1-NBMeO at a saturating concentration of 1 nM in a 600-μl reaction volume of binding buffer containing 50 mM Tris and 10 mM $MgCl_2$, pH 7.4. Nonspecific binding was determined in the presence 100 μM mianserin (Tocris Cookson, Ellisville, MO).

Fluorescence Microscopy. For fluorescence microscopic analysis of receptor subcellular localization, HEK293T cells were grown on coverslips precoated with poly(L-lysine) in six-well plates and transfected with 500 ng of GFP-tagged receptors. For colocalization of GFP-tagged receptors with the ER marker DsRed2-ER, HEK293T cells grown on coverslips were transfected with 500 ng of GFP-tagged receptors and 300 ng of pDsRed2-ER. The cells were fixed with 4% paraformaldehyde-4% sucrose mixture in phosphate-buffered saline for 15 min and stained with 4,6-diamidino-2-phenylindole for 5 min. The coverslips were mounted, and fluorescence was detected with a Leica DMRA2 epifluorescent microscope as described previously (Wu et al., 2003; Dong and Wu, 2006). Images were deconvolved using SlideBook software and the nearest neighbor deconvolution algorithm (Intelligent Imaging Innovations, Denver, CO).

Structural Analysis of the F(X)$_6$LL Motif in β_2-AR and α_{2B}-AR. A model of the α_{2B}-AR was constructed using the newly published high-resolution crystal structure of human β_2AR (Protein Data Bank code 2rh1) (Cherezov et al., 2007; Rosenbaum et al., 2007). The sequence of α_{2B}-AR was threaded onto the β_2-AR/T4-lysozyme chimera structure based on a sequence alignment generated in Clustal W. The alignment of the 7 TMs in addition to the eighth helix of the cytosolic C-terminal domain were ensured manually using DeepView/Swiss PDB viewer. The Swiss-model workspace was then used to submit the file to the Swiss-model automated structure homology-modeling server under "project optimize mode" for energy minimization (Arnold et al., 2006). The resulting file was then loaded into PyMOL to generate detailed renderings of the model. The Protein Data Bank file 2rh1 was directly loaded into PyMOL to generate detailed images of the structure of the human β_2-AR.

Coimmunoprecipitation of α_{2B}-AR and ER Chaperones. HEK293T cells cultured on 100-mm dishes were transfected with GFP-tagged α_{2B}-AR or its mutants for 48 h. The cells were washed twice with phosphate-buffered saline, harvested, and lysed with 500 μl of lysis buffer containing 50 mM Tris-HCl, pH 7.4, 150 mM NaCl, 1% Nonidet P-40, 0.5% sodium deoxycholate, 0.1% SDS, and Complete Mini protease inhibitor cocktail. After gentle rotation for 1 h at 4°C, the samples were centrifuged for 15 min at 14,000*g*, and the supernatant was incubated with 50 μl of protein G-Sepharose for 1 h at 4°C to remove nonspecific bound proteins. The samples were then incubated with 5 μg of anti-GFP antibodies overnight at 4°C with gentle rotation followed by an incubation with 50 μl of protein G-Sepharose beads for 5 h as described previously (Dong and Wu, 2006). After the resin was collected and washed two times with lysis buffer without SDS, 100 μl of 2× SDS-PAGE loading buffer was added to the beads and boiled in a Spin-Prep Column (Sigma-Aldrich) for 10 min. Thirty microliters from each sample was then separated by SDS-PAGE to probe for calnexin and calreticulin in the GFP immunoprecipitates by immunoblotting. In parallel, each sample was further diluted five times with 1× SDS-PAGE loading buffer, separated by SDS-PAGE, and probed with GFP antibody to determine the amount of the receptor in the immunoprecipitates.

Chemical and Low-Temperature Rescue. HEK293T cells were cultured in six-well dishes and transfected with GFP-tagged α_{2B}-AR for 24 h as described above. The cells were incubated with DMSO at a concentration of 2% in a total of 2 ml of DMEM without fetal bovine serum for an additional 24 h. For low-temperature rescue, the cells were cultured at 30°C for 24 h as described previously (Dong and Wu, 2006). The cell-surface expression of α_{2B}-AR was then measured by ligand binding in intact live HEK293T cells using [^{3}H]RX821002 as described above.

Measurement of cAMP Production. cAMP concentrations were measured by using cAMP enzyme immunoassay system (Biotrak; GE Healthcare, Chalfont St. Giles, Buckinghamshire, UK) as described previously (Filipeanu et al., 2006; Dong and Wu, 2007). HEK293T cells were cultured in 100-mm dishes and transfected with 3 μg of β_2-AR or its mutants tagged with GFP. After 6 h, the cells were split into 12-well plates and cultured for 12 h. The cells were then starved for 24 h and then incubated with isobutyl methylxanthine (0.1 mM) for 30 min before stimulation with ISO at a concentration of 10 μM for 5 min at room temperature. The reactions were stopped by aspirating the medium, and the cells were lysed using 200 μl of dodecyltrimethylammonium (2.5%). One hundred microliters of cell lysate was transferred into microtiter plates and incubated with anti-cAMP antiserum, followed by the incubation with cAMP-peroxidase conjugate. After washing and addition of substrate, peroxidase activity was measured by spectrometry.

Measurement of ERK1/2 Activation. HEK293T cells cultured on six-well dishes were transfected for 36 to 48 h. The cells were then starved for at least 3 h before stimulation with the agonist UK14304 at a concentration of 1 μM for 5 min as described previously (Wu et al., 2003). The stimulation was terminated by the addition of 300 μl of 1× SDS gel loading buffer. After solubilization of the cells, 20 μl of sample was separated by 12% SDS-PAGE. Activation of ERK1/2 was determined by measuring the level of ERK1/2 phosphorylation with a phosphospecific ERK1/2 antibody. Blots were then stripped and reprobed with total ERK1/2-specific antibodies to confirm equal loading.

Immunoblotting. Western blot analysis of protein expression was carried out as described previously (Wu et al., 2003; Dong and Wu, 2007). HEK293T cell lysates were separated by SDS-PAGE and transferred onto polyvinylidene difluoride membranes. The signal was detected using ECL Plus (PerkinElmer Life and Analytical Sciences) and a Fuji Film luminescent image analyzer (LAS-1000 Plus; Fuji, Tokyo, Japan) and quantitated using the Image Gauge program (version 3.4).

Statistical Analysis. Differences were evaluated using Student's *t* test, and $P < 0.05$ was considered statistically significant. Data are expressed as the mean ± S.E.

Results

The F(X)$_6$LL Motif Is Required for the ER Export and Cell Surface Transport of α_{2B}-AR, AT1R, α_{1B}-AR, and β_2-AR. We have demonstrated previously that mutation of the Phe and LL residues spaced by six residues [F(X)$_6$LL] in the membrane proximal CT (Fig. 1A) markedly block the cell-surface expression of α_{2B}-AR and AT1R as measured by ligand binding of membrane preparations and subcellular distribution of the receptors (Duvernay et al., 2004). To further confirm the function of the F(X)$_6$LL motif in mediating their transport to the cell surface, α_{2B}-AR and AT1R and their mutants (α_{2B}-ARm and AT1Rm) in which the Phe and LL residues in the F(X)$_6$LL motif were mutated to alanines, were transiently expressed in HEK293T cells, and the cell-surface expression of the receptors were measured by ligand binding in intact live cells, which will accurately measure the number of receptors at the plasma membrane and eliminate possible contamination with intracellular organelles of membrane preparations. The cell-surface expression of α_{2B}-ARm and AT1Rm were dramatically reduced by 88 and 91%, respectively, compared with their wild types (Fig. 1B). In contrast, mutation of the F(X)$_6$LL motif did not significantly alter the overall receptor expression (Fig. 1B). These data are consistent with our previous data demonstrating an essential role of the F(X)$_6$LL motif in α_{2B}-AR and AT1R transport to the cell surface.

Because the F(X)$_6$LL motif is highly conserved in many family A GPCRs (Fig. 1A) (Duvernay et al., 2004), we then asked whether the F(X)$_6$LL motif is also important for ER export of α_{1B}-AR and β_2-AR. Similar to the effect on the

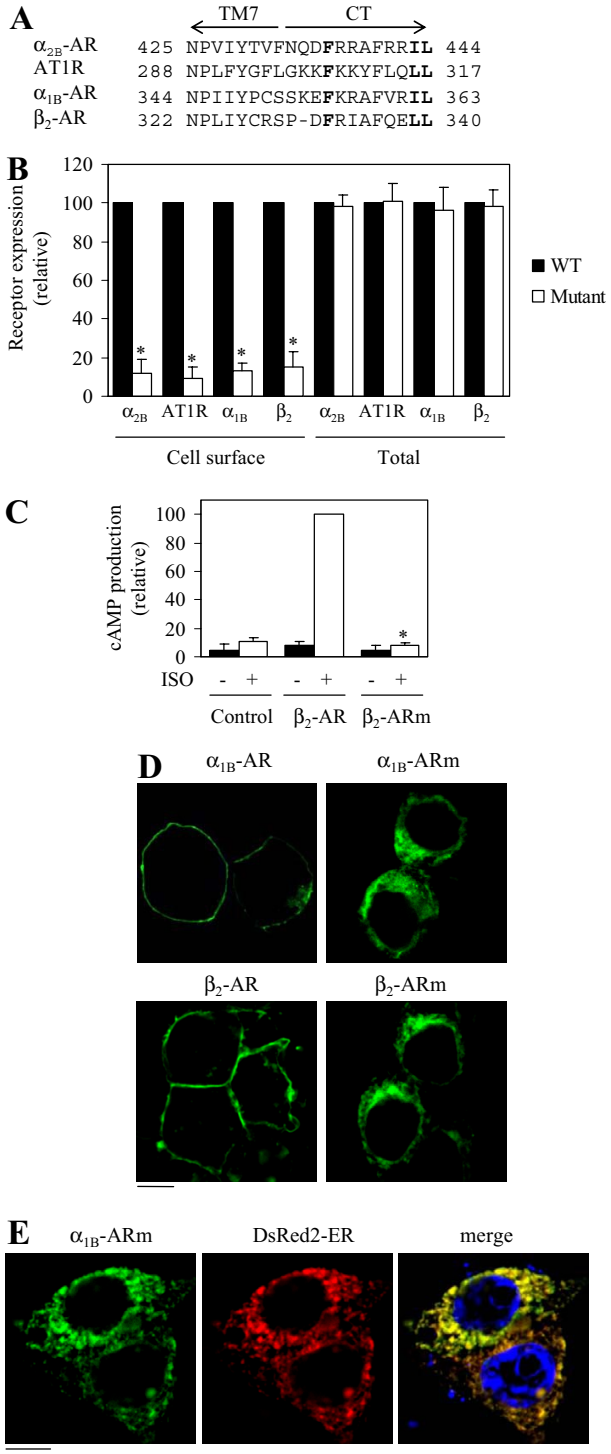

Fig. 1. Effect of the mutation of the $F(X)_6LL$ motif on the transport of α_{2B}-AR, AT1R, α_{1B}-AR, and β_2-AR to the cell surface. A, a sequence alignment of the membrane-proximal CT regions of α_{2B}-AR, AT1R, α_{1B}-AR, and β_2-AR carrying the $F(X)_6LL$ motif. The Phe and LL residues spaced by six residues are in boldface type. TM7, seventh transmembrane domain. B, quantification of the cell surface and total expression of α_{2B}-AR, AT1R, α_{1B}-AR, and β_2-AR and their mutants (α_{2B}-ARm, AT1Rm, α_{1B}-ARm, and β_2-ARm) in which the $F(X)_6LL$ motif was mutated. HEK293T cells cultured on six-well plates were transfected with each of the receptors and then split onto 12-well plates. The cell-surface expression of α_{2B}-AR, AT1R, α_{1B}-AR, and β_2-AR was measured by intact cell binding assays using [^{3}H]RX821002, ^{125}I-Ang II, [7-methoxy-^{3}H]prazosin, and [^{3}H]CGP12177, respectively, as described under *Materials and Methods*. The mean values of specific ligand binding from cells transfected with α_{2B}-AR, α_{2B}-ARm, AT1R, AT1Rm, α_{1B}-AR, α_{1B}-ARm, β_2-AR, and β_2-ARm were 23,327 ± 591, 2799 ± 126, 9734 ± 342, 876 ± 155, 31,142 ± 963, 4048 ± 625, 38,560 ± 2432, and 5784 ± 289 cpm, respectively. Total receptor expression was determined by flow cytometry measuring the GFP signal as described under *Materials and Methods*. The data shown are percentages of the mean value obtained from cells transfected with wild-type receptors and are presented as the mean ± S.E. of at least three separate experiments. *, $p < 0.05$ versus cells transfected with wild-type receptors. C, cAMP production in cells expressing β_2-AR and β_2-ARm. HEK293T cells were cultured on six-well plates and transfected with the pEGFP-N1 vector (GFP), GFP-tagged β_2-AR, or β_2-ARm. The cells were then stimulated with ISO at a concentration of 10 μM for 5 min. cAMP production was measured as described under *Materials and Methods*. The data shown are expressed as percentages of the cAMP production obtained in cells transfected with β_2-AR and stimulated with ISO and presented as the mean ± S.E. of three separate experiments. In a typical experiment, the cAMP concentration after stimulation with ISO in cells expressing wild-type β_2-AR is 2331 fmol/well. *, $p < 0.05$ versus cells transfected with β_2-AR. D, subcellular localization of β_2-AR and α_{1B}-AR and their mutants. GFP-conjugated wild-type and mutated receptors were transiently expressed in HEK293T cells, and their subcellular distribution was revealed by fluorescence microscopy as described under *Materials and Methods*. E, colocalization of α_{1B}-ARm with the ER marker DsRed2-ER. HEK293T cells were cotransfected with the GFP-tagged α_{1B}-ARm together with the plasmid pDsRed2-ER, and the subcellular distribution and colocalization of the receptor with DsRed2-ER were revealed by fluorescence microscopy as described under *Materials and Methods*. Green, α_{1B}-AR tagged with GFP; red, the ER marker DsRed2-ER; yellow, colocalization of the receptor with the ER; blue, DNA staining by 4,6-diamidino-2-phenylindole (nuclei). The data shown in D and E are representative images of at least three independent experiments. Scale bar, 10 μm.

transport of α_{2B}-AR and AT1R, mutation of the Phe356 and Ile362/Leu363 residues in α_{1B}-AR (α_{1B}-ARm) and mutation of Phe332 and Leu339/Leu340 in β_2-AR (β_2-ARm) inhibited their cell surface expression by 87 and 85%, respectively, without altering total receptor expression compared with wild-type receptors (Fig. 1B). Consistent with the dramatic attenuation of cell-surface expression, cAMP production in response to stimulation of ISO was markedly inhibited in cells expressing β_2-ARm compared with cells expressing wild-type β_2-AR (Fig. 1C).

Analysis of the subcellular localization of the receptors by fluorescence microscopy showed that α_{1B}-ARm and β_2-ARm were unable to reach the cell surface and were extensively accumulated in the perinuclear region (Fig. 1D). To further evaluate whether the $F(X)_6LL$ motif modulates α_{1B}-AR transport at the level of the ER, α_{1B}-AR and its mutant were expressed together with the ER marker DsRed2-ER, and their colocalization was then analyzed. As anticipated, α_{1B}-AR did not significantly colocalize with DsRed2-ER and was expressed at the cell surface, which was confirmed by colocalization with tetramethylrhodamine-conjugated concanavalin A, a plasma membrane marker (data not shown). In contrast, α_{1B}-ARm was strongly colocalized with the ER marker DsRed2-ER (Fig. 1E). Similar results were obtained in cells transfected with β_2-ARm (data not shown). These data suggest that the $F(X)_6LL$ motif may function as a common signal dictating ER export of multiple GPCRs.

Effect of Substitution of the Phe and LL Residues in the $F(X)_6LL$ Motif with Other Hydrophobic Residues on α_{2B}-AR Transport to the Cell Surface. To determine the physiochemical requirements for the Phe and LL residues to perform their functions in mediating GPCR export from the ER, we mutated the Phe and LL residues in the $F(X)_6LL$ motif of α_{2B}-AR to different hydrophobic residues. Each mutation's ability to substitute for the Phe and LL residues was determined by measuring cell-surface receptor

expression by intact cell ligand binding and subcellular distribution. Mutation of the Phe436 residue to Val, Leu, Trp, and Tyr significantly impaired α_{2B}-AR transport to the cell surface (Fig. 2A). Phe436 is substituted best by Tyr with ligand binding at 32% of α_{2B}-AR. F436V, F436L, and F436W mutants bound ligand less than 15% that of α_{2B}-AR (Fig. 2A). Consistent with ligand binding, subcellular distribution analysis showed that F436Y partially expressed at the cell surface, whereas the majority of the F436V, F436L, and F436W mutants were retained inside the cell (Fig. 2B). Likewise, mutation of the Ile443/Leu444 residues to dihydrophobic VV and FF residues also markedly impeded α_{2B}-AR export to the cell surface, as revealed by intact cell ligand biding (Fig. 2A) and subcellular localization (Fig. 2B). These results indicate that the role of the Phe436 and Ile443/Leu444 residues can not be fully substituted by other hydrophobic residues and suggest that Phe436 and Ile443/Leu444 have unique properties that are required for proper modulation of export from the ER of newly synthesized α_{2B}-AR.

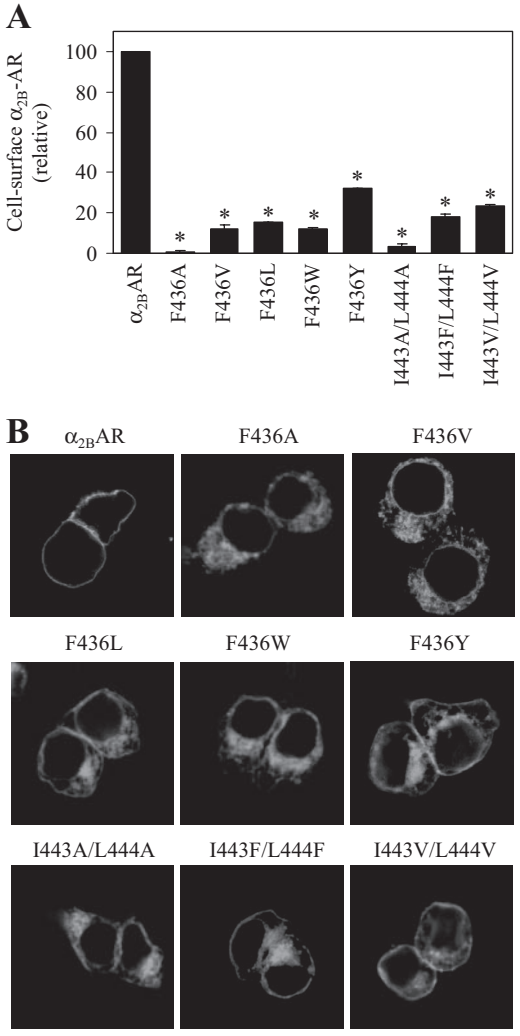

Fig. 2. Effect of substitution of Phe436 and Ile443/Leu444 with different hydrophobic residues on α_{2B}-AR transport to the cell surface. A, specific [^{3}H]RX821002 binding on intact HEK293T cells transfected with α_{2B}-AR and its mutants. HEK293T cells cultured on six-well plates were transfected with GFP-conjugated α_{2B}-AR or individual mutants. The cell-surface expression of the receptors was measured by intact cell ligand binding as described under *Materials and Methods*. The data are presented as the percentage of specific binding from cells transfected with α_{2B}-AR and are presented as the mean ± S.E. of three separate experiments. *, $p < 0.05$ versus cells transfected with α_{2B}-AR. B, subcellular localization of α_{2B}-AR and its mutants revealed by detecting GFP fluorescence.

Structural Analysis of the F(X)$_6$LL Motif in β_2-AR and α_{2B}-AR. To provide insights into the molecular mechanism underlying the function of the F(X)$_6$LL motif in regulating GPCR trafficking, we first study how the Phe and LL residues in the F(X)$_6$LL motif are presented within the newly published high-resolution crystal structure of β_2-AR (Cherezov et al., 2007; Rosenbaum et al., 2007). The C terminus of β_2-AR forms an amphipathic α-helix (also known as helix 8) that projects from the seventh TM, parallel to the membrane itself. It is terminated with a cysteine residue anchoring the helix to the membrane. The side chains of the Phe332 and Leu339/Leu340 residues project from the same face of the amphipathic α-helix back toward the membrane. However, the side chains of the Phe332 and Leu339/Leu340 are surrounded by quite distinct environments (Fig. 3A). The bulky, aromatic side chain of Phe332 seems to be buried within the hydrophobic core of the receptor. In contrast, the branched carbon side chains of the Leu339/Leu340 residues seem to be in a more accessible region of the receptor (Fig. 3A). A surface map of the receptor indicates the solvent accessibility of the entire receptor structure in blue and any solvent accessibility for Phe332 or Leu339/Leu340 in yellow. From the model it is clear that most of the Leu339/Leu340 side chains are exposed to the cytosolic space in the receptor's native environment. The side chain of Phe332, on the other hand, displays very little solvent accessibility (Fig. 3A). Close examination of the Phe332 residue reveals that its side chain is cradled by the hydrophobic residue Ile58 in the juxtamembrane portion of the TM1 (Fig. 3B).

We then constructed a homology model of α_{2B}-AR based on the crystal structure of β_2-AR (Cherezov et al., 2007; Rosenbaum et al., 2007). An accompanying alignment shows the high level of sequence homology in the C termini between α_{2B}-AR and β_2-AR (Fig. 1A). The positions of the Phe436 and Ile443/Leu444 residues in the F(X)$_6$LL motif of α_{2B}-AR are exactly same as those in the β_2-AR (Fig. 3C), and the Phe436 residue is in close proximity to the Val42 residue in the TM1 (Fig. 3D). These data suggest a possible intramolecular interaction between the Phe332 and Ile58 residues in β_2-AR and between the Phe436 and Val42 residues in α_{2B}-AR.

Effect of Mutating Ile58 and Val42 on the Cell Surface Expression, Subcellular Localization, and Signaling of β_2-AR and α_{2B}-AR. To test the possible contribution of the Ile58 and Val42 residues to the trafficking of β_2-AR and α_{2B}-AR, we first determined the effect of mutating Ile58 and Val42 to alanines on the transport to the cell surface of β_2-AR and α_{2B}-AR, respectively. Wild-type receptors and their mutants were transiently expressed in HEK293T cells, and their expression at the cell surface was quantified by intact cell ligand binding and subcellular distribution as revealed by fluorescence microscopy. The cell surface expression of the I58A and V42A mutants was markedly attenuated by 90 and 61%, respectively, compared with their wild-type counterparts (Fig. 4A).

We then determined the effect of mutation of the residue Val78, which is analogous to Val42 in α_{2B}-AR, on the transport of 5-HT$_{2C}$ receptor. In contrast to α_{2B}-AR, AT1R, α_{1B}-AR, and β_2-AR, which have the F(X)$_6$LL motif in the C

termini, 5-HT_{2C} receptor possesses the $Y(X)_6YL$ motif in the C terminus. Because the 5-HT_{2C} receptor ligand [^{3}H]1-NB-MeO has been well characterized in a binding assay of membrane preparations, we determined the effect of mutating the residue Val78 on ligand binding of the 5-HT_{2C} receptor in the membrane preparations and compared with the α_{2B}-AR mutant V42A. Consistent with intact cell ligand binding, ligand binding of membrane preparations from cells expressing the mutant V42A was much lower than from cells expressing wild-type α_{2B}-AR (Fig. 4B). In contrast, mutation of Val78 to alanine significantly enhanced ligand binding of 5-HT_{2C} receptor in membrane preparations (Fig. 4B). Total receptor expression measured by flow cytometric analysis of the GFP signal showed no significant difference between wild-type and mutated receptors (data not shown). Consistent with the ligand binding data, subcellular distribution analysis revealed that the I58A mutant was completely unable to transport to the cell surface, and the V42A mutant displayed a substantial intracellular retention, whereas the V78A mutant robustly expressed at the cell surface (Fig. 4C).

We then determined whether mutation of Val42 could influence receptor signaling by measuring ERK1/2 activation. Consistent with a significant reduction in the cell surface receptor expression as measured by ligand binding and subcellular localization, ERK1/2 activation by UK14304 in cells expressing the V42A mutant was clearly attenuated compared with cells expressing wild-type α_{2B}-AR (Fig. 4D). These data further indicate that the Val42 residue is important for the cell surface transport of α_{2B}-AR. These data also suggest that the hydrophobic residues (such as Val42) in the TM1 are essential for receptor export to the cell surface, which may serve as a contact point for the Phe residue in the C-terminal $F(X)_6LL$ motif to coordinate tertiary structure of the receptor.

To further define the role of the possible interaction be-

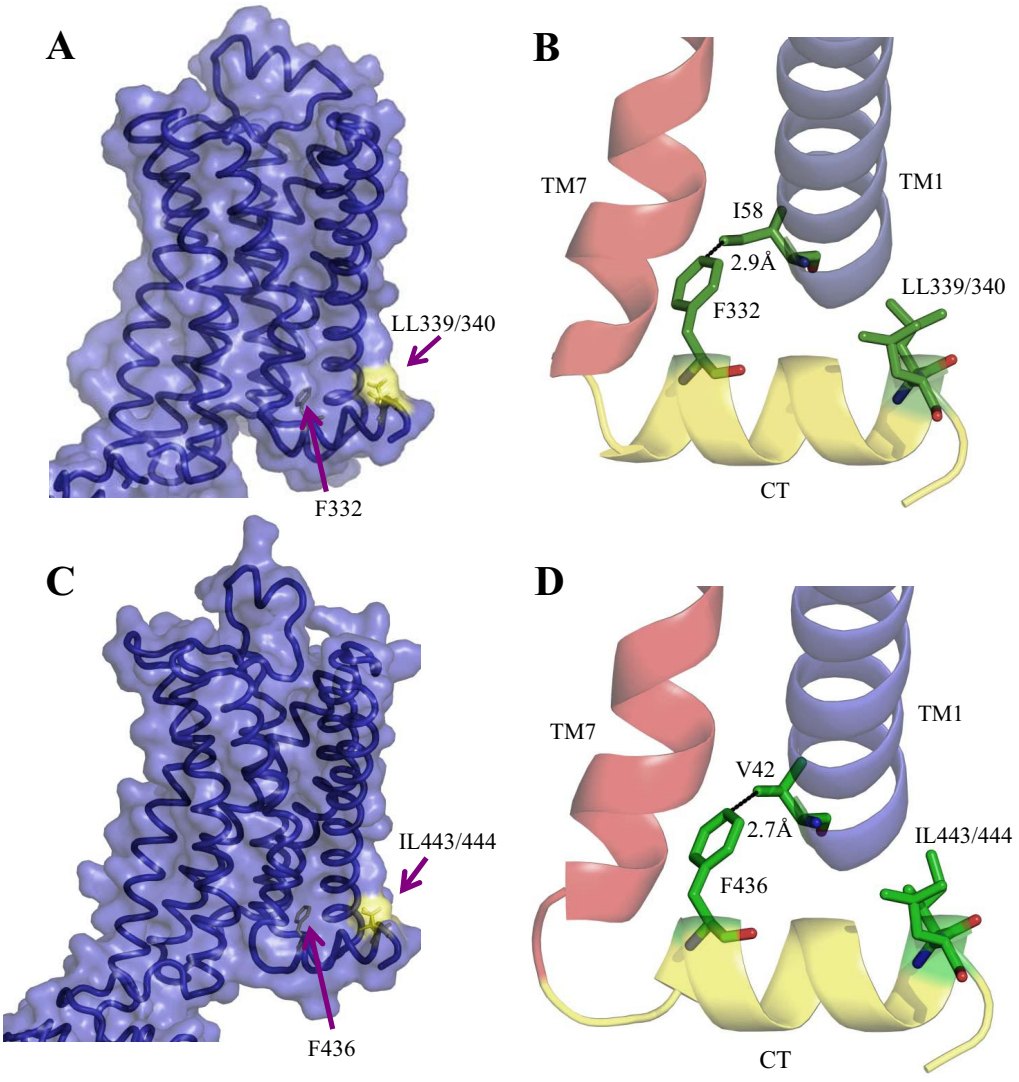

Fig. 3. Structural analysis of the $F(X)_6LL$ motif in β_2-AR and α_{2B}-AR. A, representation of the "Connelly surface" or the surface traced out by water molecules interacting with exposed portions of the protein based on the crystal structure of β_2-AR. The Connelly surface for the entire protein is represented in blue. Those portions of Phe332 and Leu339/Leu340 with the potential for interaction with water molecules are shown in yellow. B, a close view of the Phe332 and Leu339/Leu340 residues and their intramolecular environments. TM1 is colored in blue, TM7 in red, and CT in yellow. Carbon, oxygen, and nitrogen in residues are labeled in green, red, and blue, respectively. The distance between Phe332 of the C terminus and Ile58 of the first transmembrane domain is labeled in angstroms. C, homology modeling of α_{2B}-AR based on the crystal structure of β_2-AR as in A. D, positions of the Phe436, Ile443/Leu444, and Val42 residues and their intramolecular environments in α_{2B}-AR as in B for β_2-AR.

tween Val42 and Phe436 in α_{2B}-AR maturation, we examined the effect of simultaneously mutating Val42 to Phe and Phe436 to Val on the cell surface expression of α_{2B}-AR. Individual mutation of Val42 to Phe or Phe436 to Val markedly attenuated α_{2B}-AR cell surface expression (Fig. 4E). Interestingly, the cell surface expression of double mutant V42F/F436V was significantly higher than individual mutants V42F and F436V (Fig. 4E). These data suggest that swapping

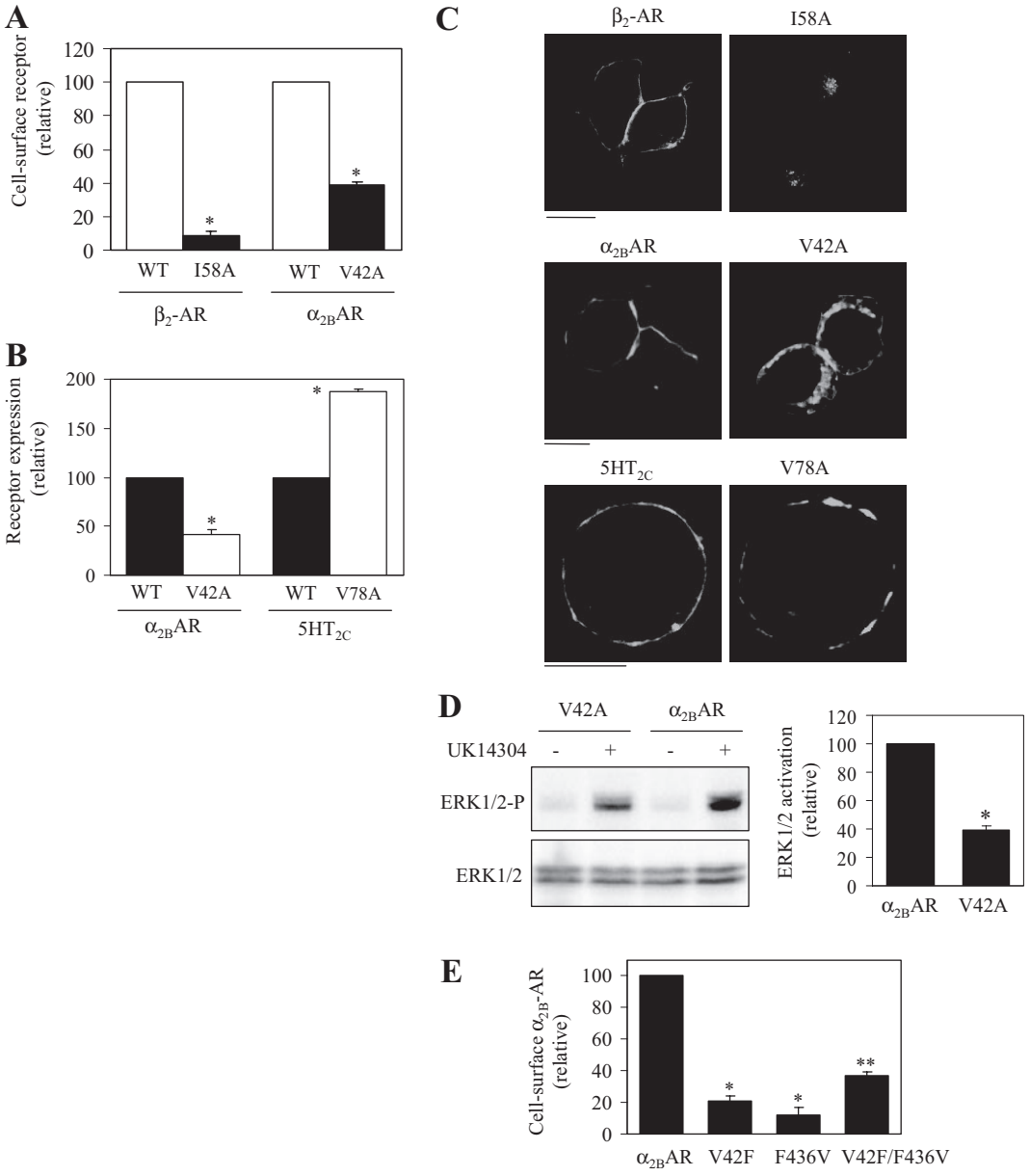

Fig. 4. Effect of mutation of the Ile58, Val42, and Val78 residues on the cell surface transport and subcellular localization of β_2-AR, α_{2B}-AR, and 5-HT_{2C} receptor, respectively. A, quantitation of the cell-surface expression of β_2-AR and α_{2B}-AR and their mutants. HEK293T cells cultured on six-well plates were transfected with GFP-conjugated receptors and then split onto 12-well plates. The cell-surface expression of the receptors was measured by intact cell binding assays as described under *Materials and Methods*. The mean values of specific ligand binding were 37,843 ± 844, 3238 ± 289, 23,663 ± 597, and 9254 ± 200 cpm from cells transfected with β_2-AR, I58A, α_{2B}-AR, and V42A, respectively. The data shown are the percentage of the mean value obtained from cells transfected with wild-type (WT) receptor and are presented as the mean ± S.E. of three experiments. B, specific ligand binding to membrane fractions prepared from the cells transfected with α_{2B}-AR and 5-HT_{2C} receptor and their mutants. HEK293T cells were transiently transfected with GFP-tagged α_{2B}-AR, 5-HT_{2C} receptor, or their mutants (V42A and V78A). The membrane fractions were incubated with the radioligands [^{3}H]RX-821002 or [^{3}H]1-NBMeO as described under *Materials and Methods*. The mean values of specific ligand binding were 22,324 ± 1102, 9376 ± 1116, 10,196 ± 660, and 19,085 ± 312 cpm (mean ± S.E., n = 3–4) from cells transfected with α_{2B}-AR, V42A, 5-HT_{2C} receptor, and V78A, respectively. C, subcellular distribution of β_2-AR, α_{2B}-AR, and 5-HT_{2C} receptor and their mutants. HEK293T cells transfected with GFP-conjugated receptors were split onto coverslips, and subcellular distribution of the receptors was revealed by detecting GFP fluorescence as described under *Materials and Methods*. The data are representative images of at least four independent experiments. Scale bar, 10 μm. C, ERK1/2 activation by α_{2B}-AR and its mutant. HEK293T cells cultured on six-well plates were transfected with α_{2B}-AR or V42A and stimulated with UK14304 at a concentration of 1 μM for 5 min. ERK1/2 activation was determined by Western blot analysis using phosphospecific ERK1/2 antibodies. Top, left, a representative blot of ERK1/2 activation; bottom, left, total ERK1/2 expression; Right, quantitative data expressed as the percentage of the ERK1/2 activation obtained from cells transfected with α_{2B}-AR and are presented as the mean ± S.E. of three separate experiments. E, quantitation of the cell-surface expression of α_{2B}-AR and their mutants V42F, F436V, and V42F/F436V. *, $p < 0.05$ versus cells transfected with their respective wild-type receptors; **, $p < 0.05$ versus cells transfected with V42F or F436V.

Val42 in the TM1 and Phe436 in the C terminus may partially rescue α_{2B}-AR transport.

The Residues Valine and Isoleucine Are Conserved in the TM1s of GPCRs Carrying the F(X)$_6$LL Motif in the C Termini. Because we have demonstrated that the F(X)$_6$LL is highly conserved in the family A GPCRs and that the Phe residue in the motif probably interacts with the hydrophobic residue Ile58 in β_2-AR and Val42 in α_{2B}-AR, we then searched the GPCR database to determine whether the Ile and Val residues are conserved among the GPCRs carrying the F(X)$_6$LL motif in the C termini. As shown in Fig. 5, of a total of 43 human GPCRs having the F(X)$_6$LL motif in the C termini, 39 receptors (91%) have the residues Ile/Leu/Val in the TM1 in the position of Ile58 in β_2-AR and Val42 in α_{2B}-AR (Fig. 5, A and B). Among these GPCRs, 21 receptors (49%) have either Ile (16 receptors) or Leu residues (5 receptors) (Fig. 5A), and 18 GPCRs (42%) have Val residue (Fig. 5B). Only four GPCRs (9%) with the F(X)$_6$LL motif have Phe (three receptors) and His residues (one receptor) (Fig. 5C). These data strongly indicate that the hydrophobic residues Ile/Leu and Val are also highly conserved among GPCRs carrying the F(X)$_6$LL motif. These data further support the important role of the potential interaction between the Val/Ile/Leu residues in the TM1 and the Phe residue in the C termini in modulating GPCR trafficking.

Differential Interaction of the α_{2B}-AR Mutants F436A and I443A/L444A with ER Chaperone Proteins. To further determine whether the Phe436 and Ile443/Leu444 residues in the F(X)$_6$LL motif are differentially involved in GPCR folding, we compared the interaction of α_{2B}-AR and its mutants F436A and I443A/L444A with the ER chaperones calnexin and calreticulin. Within the ER, molecular chaperones bind to nascent proteins and facilitate their proper folding. Properly folded receptors are released for export, whereas misfolded proteins remain bound to the chaperone and are eventually targeted for degradation. Therefore, terminally misfolded receptors will display extended and robust interactions with the chaperones (Lu et al., 2003; Ulloa-Aguirre et al., 2004; Robert et al., 2005; Apaja et al., 2006). The GFP-tagged α_{2B}-AR and its mutants were transiently expressed in HEK293T cells, and the receptors were then immunoprecipitated with anti-GFP antibodies. The ER chaperones calnexin and calreticulin in the GFP immunoprecipitates were analyzed by immunoblotting. To exclude the possibility that receptor interaction with ER chaperones induced by misfolding of the receptors was caused by a higher level of the receptors, wild-type and mutated α_{2B}-AR were transiently expressed in HEK293 cells using 10 times less of the plasmid DNA. A significant amount of both calnexin and calreticulin was immunoprecipitated by GFP antibodies from cells expressing α_{2B}-AR (Fig. 6), consistent with the interaction of many GPCRs with ER chaperones (Lu et al., 2003; Robert et al., 2005; Apaja et al., 2006), confirming that chaperone interaction is a normal process in GPCR biogenesis. Interestingly, the amount of chaperones detected in the GFP immunoprecipitates from cells expressing the mutant F436A was significantly higher than from cells expressing α_{2B}-AR but remained the same from cells expressing the I443A/L444A mutant (Fig. 6A). The amount of the α_{2B}-AR plasmid DNA used in transient transfection did not clearly alter the receptor interaction with the ER chaperones (Fig. 6). These data indicate that the F436A mutant displays a stronger,

A GPCRs with I/L and F(X)$_6$LL

	TM1	CT
β_1-AR	NVLVIVA**I**AKTPRLQT	NPIIYCRS-PD**F**RKAFQR**LL**CCAR
β_2-AR	NVLVITA**I**AKFERLQT	NPLIYCRS-PD**F**RIAFQE**LL**CLRR
β_3-AR	NLLVIVA**I**AWTPRLQT	NPLIYCRS-PD**F**RSAFRR**LL**CRCG
D5DR	NVLVCAA**I**VRSRHLRA	NPVIYA-FNAD**F**QKVFAQ**LL**GCSH
5HT1E	NLAVIMA**I**GTTKKLHQ	NPLLYTSFNED**F**KLAFKK**LI**RCRE
TAAR2	NLAMIIS**I**SYFKQLHT	NPLIYGFFYPW**F**RRALKY**IL**LGKI
ACM2	NILVMVS**I**KVNRHLQT	NPACYALCNAT**F**KKTFKH**LL**MCHY
ACM4	NILVMLS**I**KVNRQLQT	NPACYALCNAT**F**KKTFRH**LL**LCQY
AT1R	NSLVVIV**I**YFYMKLKT	NPLFYGFLGKK**F**KRYFLQ**LL**KYIP
CXCR1	NSLVMLV**I**LYSRVGRS	NPIIYAFIGQN**F**RHGFLK**IL**AMHG
CXCR2	NSLVMLV**I**LYSRVGRS	NPLIYAFIGQK**F**RHGLLK**IL**AIHG
CXCR5	N-VLVLV**I**LERHRQTR	NPMLYTFAGVK**F**RSDLSR**LL**TKLG
PRLHR	NCLLVLV**I**ARVRRLHN	NPFIYAWLHDS**F**REELRK**LL**VAWP
P2Y6	NICVITQ**I**CTSRRALT	DPILFYFTQKK**F**RRRPHE**LL**QKLT
SS1R	NSMVIYV**I**LRYAKMKT	NPILYGFLSDN**F**KRSFQR**IL**CLSW
GPR8	NTAVILV**I**LRAPKMKT	NPFLYAFLDDN**F**RKNFRS**IL**RC
CXCR3	NGAVAAV**LL**SRRTALS	NPLLYAFVGVK**F**RERMWM**LL**LRLG
GPR7	NSAVLYV**LL**RAPRMKT	NPFLYAFLDAS**F**RRNLRQ**LI**TCRA
LSHR	NMTVLFV**LL**TSRYKLT	NPFLYAIFTKT**F**QRDFFL**LL**SKFG
TSHR	NVFVLLI**LL**TSHYKLN	NPFLYAIFTKA**F**QRDVFI**LL**SKFG
FSHR	NIIVLVI**LL**TTSQYKLT	NPFLYAIFTKN**F**RRDFFI**LL**SKCG

B GPCRs with V and F(X)$_6$LL

5HT1A	NILVILS**V**ACNRHLRT	NPIIYPCSSKE**F**KRAFMR**IL**GCQC
α_{1B}-AR	NILVILS**V**ACNRHLRT	NPIIYPCSSKE**F**KRAFVR**IL**GCQC
α_{1D}-AR	NLLVILS**V**ACNRHLQT	NPLIYPCSSRE**F**KRAFLR**LL**RCQC
DRD1	NTLVCAA**V**IRFRHLRS	NPIIYA-FNAD**F**RKAFST**LL**GCYR
5HT4R	NLLVMVA**V**CWDRQLRK	NPFLYAFLNKS**F**RRAFLI**IL**CCDD
5HT1B	NAFVIAT**V**YRTRKLHT	NPIIYTMSNED**F**KQAFHK**LI**RFKC
α_{2A}-AR	NVLVIIA**V**FTSRALKA	NPVIYTIFNHD**F**RRAFKK**IL**CRGD
α_{2B}-AR	NALVILA**V**LTSRSLRA	NPVIYTIFNQD**F**RRAFRR**IL**CRPW
α_{2C}-AR	NVLVVIA**V**LTSRALRA	NPVIYTVFNQD**F**RRSFKH**IL**FRRR
D3DR	NGLVCMA**V**LKERALQT	NPVIYTTFNIE**F**RKAFLK**IL**SC
D2DR	NVLVCMA**V**SREKALQT	NPIIYTTFNIE**F**RKAFLK**IL**HC
TAAR8	NLLVMTS**V**LHFKQLHS	NPLIYALFYPW**F**RKAIKL**IL**SGDV
AA2B	NVLVCAA**V**GTANTLQT	NPIVYAYRNRD**F**RYTFHK**II**SRYL
AA2A	NVLVCWA**V**WLNSNLQN	NPFIYAYRIRE**F**RQTFRK**II**RSHV
AA3R	NVLVICV**V**KLNPSLQT	NPIVYAYKIKK**F**KETYLL**IL**KACV
ML1A	NLLVILS**V**YRNKKLRN	NAIIYGLLNQN**F**RKEYRR**II**VSLC
ML1B	NLLVILS**V**LRNRKLRN	NAIVYGLLNQN**F**RREYKR**IL**LALW
HH1R	NLLVLYA**V**RSERKLHT	NPLIYPLCNEN**F**KKTFKR**IL**HIRS

C GPCRs with F(X)$_6$LL but without V/I/L

ACM1	NLLVLIS**F**KVNTELKTV	NPMCYALCNKA**F**RDTFRL**LL**LCRW
ACM3	NILVIVS**F**KVNKQLKTV	NPVCYALCNKT**F**RTTFKM**LL**LCQC
ACM5	NVLVMIS**F**KVNSQLKTV	NPICYALCNRT**F**RKTFKM**LL**LCRW
CKRA	NGLVLAT**H**LAARRAARS	NPVLYAFLGLR**F**RQDLRR**LL**RGGS

Fig. 5. The conserved Phe/Ile/Leu in the first transmembrane domain of GPCRs. The data were constructed from http://www.gpcr.org. Only human sequences are shown. A, GPCRs containing the Ile and Leu residues in TM1 and the F(X)$_6$LL motif in the CT. B, GPCRs containing the Val residue in the TM1 and the F(X)$_6$LL motif. C, GPCRs containing the F(X)$_6$LL motif in the C termini but without Val, Ile, or Leu in the TM1. D2DR, dopamine D(2) receptor; D3DR, dopamine D(3) receptor; D5DR, dopamine D(5) receptor; 5HT1A, human 5-hydroxytryptamine 1A receptor; 5HT1E, 5-hydroxytryptamine 1E receptor; TAAR2, trace amine-associated receptor 2; ACM1, muscarinic acetylcholine receptor M1; ACM2, muscarinic acetylcholine receptor M2; ACM3, muscarinic acetylcholine receptor M3; ACM4, muscarinic acetylcholine receptor M4; ACM5, muscarinic acetylcholine receptor M5; AT1R, angiotensin II type 1 receptor; CXCR1, C-X-C chemokine receptor type 1; CXCR2, C-X-C chemokine receptor type 2; CXCR3, C-X-C chemokine receptor type 3; CXCR5, C-X-C chemokine receptor type 5; CKRA, human C-C chemokine receptor type 10; PRLHR, prolactin-releasing hormone receptor; P2Y6, P2Y purinoceptor 6; SS1R, somatostatin receptor type 1; GPR7, neuropeptides B/W receptor type 1; GPR8, neuropeptides B/W receptor type 2; LSHR, lutropin-choriogonadotropic hormone receptor precursor; TSHR, thyrotropin receptor precursor; FSHR, follicle stimulating hormone receptor precursor; AA2A, adenosine A2a receptor; AA2B, adenosine A2b receptor; AA3R, adenosine A3 receptor; HH1R, histamine H1 receptor; ML1A, melatonin type 1A receptor; ML1B, melatonin type 1B receptor.

extended interaction with calnexin and calreticulin and suggest that residue Phe436, but not residues Ile443/Leu444, may be involved in α_{2B}-AR folding.

Rescue of the F436A and I443A/L444A Mutants by Low-Temperature Culture and DMSO Treatments. To further test the hypothesis that residue Phe436 is involved in α_{2B}-AR folding, we investigated whether the F436A and I443A/L44A mutants could be differentially rescued by low-temperature culture and DMSO treatment. HEK293T cells transfected with either α_{2B}-AR or its mutants were allowed to express for 24 h before being cultured at 30°C or treated with 2% DMSO for an additional 24 h. Cell-surface expression of the receptors was then measured by intact cell ligand binding. Both treatment conditions have been shown to rescue the expression of certain mutant GPCRs (Bailey et al., 2004; Tan et al., 2004; Robben et al., 2006), presumably by increasing the conformational stability of the receptors, thereby facilitating their passage through the ER quality control system. Low-temperature culture (Fig. 7A) and DMSO treatment (Fig. 7B) were able to significantly increase expression over control conditions of the F436A and I443A/L444A mutants. Interestingly, the F436A mutant consistently showed a greater propensity to be rescued by both low-temperature culture (Fig. 7A) and DMSO treatment (Fig. 7B) than the I443A/L444A mutant. These results indicate that the F436A and I443A/L444A mutants have different phenotypes within the ER and suggest that the Phe436 and Ile443/Leu444 residues may contribute to different degrees to the assumption of an ER export-competent conformation for α_{2B}-AR.

Discussion

We have reported previously that the Phe436 and Ile443/Leu444 residues within the C terminus of α_{2B}-AR are required for its export from the ER (Duvernay et al., 2004; Zhou et al., 2006). Here, we demonstrated that 1) the $F(X)_6LL$ motif similarly modulates ER export of α_{2B}-AR, AT1R, α_{1B}-AR, and β_2-AR; 2) the function of the $F(X)_6LL$ motif in directing receptor export is dictated by their unique physiochemical properties; 3) Phe and LL are localized in distinct environments within the receptor superstructure, and Phe is in close proximity to Ile58 in β_2-AR and Val42 in α_{2B}-AR in the TM1; 4) mutation of Ile58 and Val42 markedly reduced receptor cell surface expression; 5) Ile and Val are highly conserved in the TM1 among GPCRs carrying the $F(X)_6LL$ motif; 6) α_{2B}-AR mutants F436A and I443A/L444A differentially associated with calnexin and calreticulin; and 7) low-temperature and chemical-chaperone treatments rescued the export of F436A and I443A/L444A to different degrees. These data strongly suggest that Phe in the $F(X)_6LL$ motif is prob-

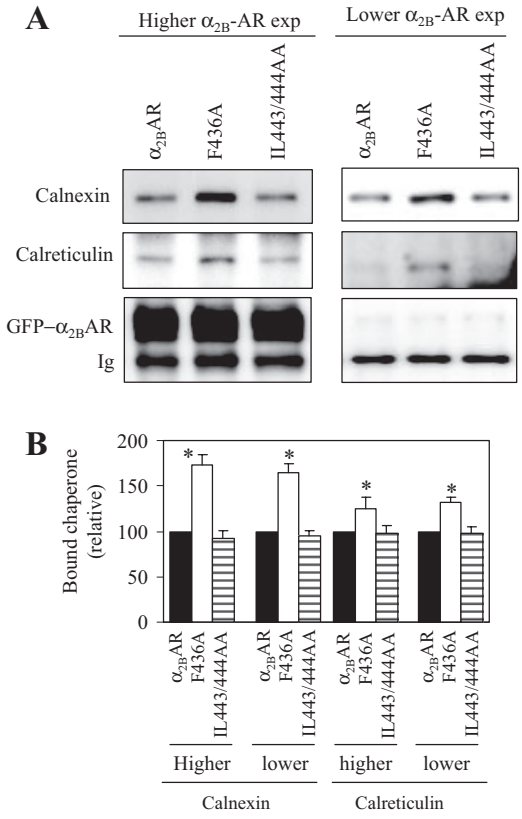

Fig. 6. Differential interaction of the α_{2B}-AR mutants F436A and I443A/L444A with ER chaperones. A, immunoblot analysis of the ER chaperones calnexin and calreticulin and α_{2B}-AR in the GFP immunoprecipitates. HEK293T cells were cultured on 10-cm dishes and then transfected with 3 μg (left) and 0.3 μg (right) of the plasmid DNA of GFP-conjugated α_{2B}-AR, F436A, or I443A/L444A, and the receptors were immunoprecipitated with anti-GFP antibodies as described under *Materials and Methods*. Calnexin (top), calreticulin (middle) and α_{2B}-AR (bottom) in the GFP immunoprecipitates were revealed by immunoblotting using antibodies against calnexin, calreticulin, and GFP, respectively. The data shown are representative of three independent experiments. B, quantitation of immunoblots from A. The data shown are the percentage of the mean value obtained from cells transfected with wild-type α_{2B}-AR and are presented as the means ± S.E. of three separate experiments. *, $p < 0.05$ versus cells transfected with wild-type α_{2B}-AR.

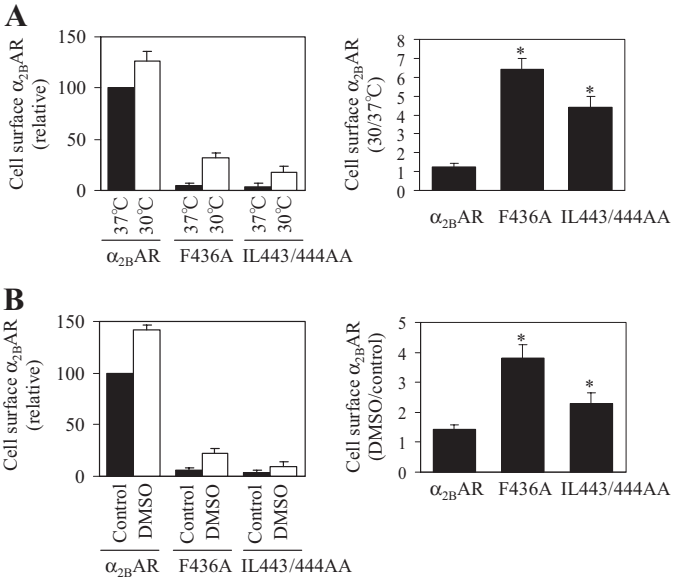

Fig. 7. Rescue of the cell-surface expression of the α_{2B}-AR mutants F436A and I443A/L444A by low-temperature culture and treatment with DMSO. A, specific [^{3}H]RX821002 binding to intact HEK293T cells transfected with α_{2B}-AR, F436A, or I443A/L444A and cultured at 37 and 30°C for 24 h. The cell-surface expression of the receptors was measured by using [^{3}H]RX821002 at a concentration of 20 nM in duplicate. Left, the data shown are -fold increase in receptor cell-surface expression at 30 and 37°C and are presented as the mean ± S.E. of three separate experiments. *, $p < 0.05$ versus wild-type α_{2B}-AR. B, specific [^{3}H]RX821002 binding to intact HEK293T cells transfected with α_{2B}-AR, F436A, or I443A/L444A and treated with 2% DMSO for 24 h. Left, the data shown are -fold increase in cell-surface receptor expression after DMSO treatment and are presented as the mean ± S.E. of three separate experiments. *, $p < 0.05$ versus wild-type α_{2B}-AR.

ably involved in receptor folding, which is mediated through hydrophobic interaction with other residues in the TM1.

We first used an intact cell ligand binding assay to determine the role of the $F(X)_6LL$ motif in the cell surface expression of four GPCRs. Our data have demonstrated that mutation of the $F(X)_6LL$ motif remarkably blocked cell surface expression of α_{2B}-AR, β_2-AR, α_{1B}-AR, and AT1R, resulting in extensive ER arrest. These data strongly suggest that the $F(X)_6LL$ motif plays a general role in modulating GPCR ER export.

It is apparent that the function of Phe436 in α_{2B}-AR export requires its unique physiochemical characteristics, including hydrophobicity, polarity, and the size of the side chain. First, Phe, Tyr, and Trp are aromatic residues with different sizes. Among them, Phe has the smallest size, and Trp has the largest size, whereas Tyr has a slightly larger size than Phe. The fact that the cell-surface transport of the mutant F436Y was much higher than the mutant F436W suggests that the size of Phe436 is likely to be the main determinant for its function. Second, the function of Phe436 could not be fully substituted by Val, Leu, Tyr, and Trp. Because Phe has the highest hydrophobicity, it is possible that the hydrophobicity of Phe436 may also play an important role in its function. Third, Phe is a nonpolar residue, and Tyr and Trp are polar residues. It is possible that the nonpolar charter of Phe436 is essential to its function. However, mutation of Phe436 to the nonpolar residues Val and Leu markedly disrupted α_{2B}-AR transport. Likewise, mutation of LL to VV and FF markedly blocked α_{2B}-AR transport, suggesting that the function of LL is dictated by its exceptional properties.

To gain insight into the molecular mechanism underlying the function of the $F(X)_6LL$ motif, we studied how Phe and LL are presented within the superstructure of β_2-AR and α_{2B}-AR using the newly published crystal structure of β_2-AR (Cherezov et al., 2007; Rosenbaum et al., 2007). Phe332 and Leu339/Leu340 in β_2-AR are surrounded by distinct environments, and Phe332 is juxtaposed with the cytosolic end of the TM1, TM2, and TM7 in a position to possibly interact with these domains. Specifically, Phe332 seems to interact with Ile58 in the TM1. The homology model of α_{2B}-AR based on the β_2-AR structure suggests that Phe436 is in close proximity to Val42. Indeed, mutation of Ile58 in β_2-AR abolished and mutation of Val42 in α_{2B}-AR markedly attenuated receptor cell surface expression. More interestingly, the cell surface transport of the double mutant V42F/F436V was significantly higher than individual mutants V42F and F436V. In contrast, mutation of Val78 in 5-HT_{2C} receptor, which does not have the $F(X)_6LL$ motif, markedly enhanced the ligand binding of 5-HT_{2C} receptor in membrane preparations. The molecular mechanism underlying this phenomenon is unknown. It is possible that mutation of Val78 facilities the transport of 5-HT_{2C} receptor, resulting in more functional receptors or enhances 5-HT_{2C} receptor's ability to bind ligand.

The inhibitory effect of Val42 mutation on α_{2B}-AR transport was not as dramatic as the Phe436 mutation, suggesting that Phe436 plays a more important role than Val42 in α_{2B}-AR export. It is possible that Phe436 may coordinate with multiple domains in addition to the TM1. In support of this concept, Fritze et al. (2003) demonstrated that the highly conserved Phe in the helix 8 of rhodopsin interacts with Tyr in the NPxxY motif, responsible for maintaining the ground state conformation of the receptor and proper realignment of the helix 8 after photoisomerization. In addition to Val42, other hydrophobic residues such as LL in the C terminus may also interact with Phe436. Nevertheless, these data suggest that Phe in the $F(X)_6LL$ motif coordinates a structural event required for the assumption of an ER export-competent conformation.

Several studies suggest that the membrane-proximal C-terminal hydrophobic residues probably modulate GPCR folding in the ER (Schulein et al., 1998; Robert et al., 2005). To further define whether Phe436 and Ile443/Leu444 are differentially involved in proper receptor folding, we first compared their interactions with calnexin and calreticulin, ER chaperone proteins that display stronger and extended interactions with misfolded GPCRs (Lu et al., 2003; Ulloa-Aguirre et al., 2004; Robert et al., 2005; Apaja et al., 2006). Our data indicate that F436A displayed higher levels of interaction with calnexin and calreticulin than I443A/L444A and wild-type α_{2B}-AR. We then compared the ability of F436A and I443A/L444A to be rescued by physical and chemical treatments. Successful rescue of misfolded GPCRs can be achieved by many approaches, such as chemical chaperones, pharmacological chaperones, and lowering temperature (Lu et al., 2003; Ulloa-Aguirre et al., 2004; Robert et al., 2005; Apaja et al., 2006). Consistent with stronger interactions of F436A with the ER chaperones, F436A had a greater propensity to be rescued by low-temperature culture and DMSO than I443A/L444A. Because the defect in ER export incurred upon mutation of Phe436 is more easily corrected with methods that presumably tighten protein conformation, we conclude that Phe436 contributes to the maintenance of proper receptor conformation to a much greater degree than Ile443/Leu444.

The function of Phe in the $F(X)_6LL$ in modulating GPCR ER export is probably mediated through interacting with other hydrophobic residues in the TM1 (e.g., Ile58 in β_2-AR and Val42 in α_{2B}-AR). Such intramolecular hydrophobic interactions have been demonstrated in many GPCRs to coordinate and maintain tertiary structure of the receptors (Fritze et al., 2003). Most interestingly, the hydrophobic residues Val/Ile/Leu are markedly conserved among GPCRs carrying the $F(X)_6LL$ motif, implying an important role played by these highly conserved hydrophobic residues in regulating GPCR function.

The Phe and LL residues in the $F(X)_6LL$ motif may dictate distinct steps involved in receptor export from the ER. Whereas our current studies suggest that Phe probably plays an important role in proper receptor folding, the precise mechanism underlying the function of LL remains unknown. Because LL is accessible to the cytosolic space, it may function as an ER export motif, which mediates receptor interaction with components of the COPII vesicles directing receptor ER export. Consistent with this possibility, the dihydrophobic residues FF mediates the ER transport of ERGIC53 and can be functionally substituted by LL. Furthermore, LL also functions as a sorting signal at the *trans*-Golgi network and at the plasma membrane (Hunziker and Fumey, 1994; Heilker et al., 1996). It is also possible that LL mediates receptor interaction with some proteins crucial for receptor ER export. Consistent with this possibility, a number of accessory proteins directly interact with the GPCR C termini to modulate receptor export (Ferreira et al., 1996; McLatchie et al., 1998).

The identification of structural determinants for GPCR export from the ER has greatly advanced our understanding of GPCR targeting to the cell surface, yet the precise mechanisms remain to be elucidated. Recent studies have also demonstrated that the transport of GPCRs beyond their export from the ER is tightly controlled at multiple transport steps along the secretory pathway (Dong et al., 2007). The regulators involved in GPCR export have just begun to be revealed. For example, we have demonstrated that the ER-to-cell surface transport of AT1R, β-AR, and α_1-AR is dependent on Rab1, Rab2, and Rab6, whereas the transport of α_{2B}-AR is dependent on Rab2 but independent of Rab1 and Rab6 (Wu et al., 2003; Filipeanu et al., 2004; Dong and Wu, 2007). We have also showed that export from the ER of different GPCRs may be differentially regulated by Sar1 (Dong et al., 2008). These data indicate that the cell surface targeting of different GPCRs may be mediated through distinct pathways. Because the efficient trafficking of GPCRs and the precise positioning of specific receptors at the cell membrane are critical aspects of integrated responses of the cell to hormones, defective GPCR transport is clearly associated with the pathogenesis of a variety of human diseases (Morello and Bichet, 2001; Conn et al., 2007). Further elucidation of the molecular mechanisms underlying the export traffic of GPCRs may provide a foundation for the development of therapeutic strategies by designing specific drugs to control GPCR biosynthesis and eventually receptor function.

Acknowledgments

We are grateful to Drs. Stephen M. Lanier, John D. Hildebrandt (Medical University of South Carolina), Kenneth P. Minneman, Kenneth E. Bernstein (Emory University), and David E. Nichols (Purdue University) for sharing reagents.

References

Apaja PM, Tuusa JT, Pietilä EM, Rajaniemi HJ, and Petäjä-Repo UE (2006) Luteinizing hormone receptor ectodomain splice variant misroutes the full-length receptor into a subcompartment of the endoplasmic reticulum. *Mol Biol Cell* **17:**2243–2255.

Arnold K, Bordoli L, Kopp J, and Schwede T (2006) The SWISS-MODEL workspace: a web-based environment for protein structure homology modelling. *Bioinformatics* **22:**195–201.

Bailey SR, Eid AH, Mitra S, Flavahan S, and Flavahan NA (2004) Rho kinase mediates cold-induced constriction of cutaneous arteries: role of alpha2C-adrenoceptor translocation. *Circ Res* **94:**1367–1374.

Bermak JC, Li M, Bullock C, and Zhou QY (2001) Regulation of transport of the dopamine D1 receptor by a new membrane-associated ER protein. *Nat Cell Biol* **3:**492–498.

Braden MR, Parrish JC, Naylor JC, and Nichols DE (2006) Molecular interaction of serotonin 5-HT2A receptor residues Phe339(6.51) and Phe340(6.52) with superpotent *N*-benzyl phenethylamine agonists. *Mol Pharmacol* **70:**1956–1964.

Cherezov V, Rosenbaum DM, Hanson MA, Rasmussen SG, Thian FS, Kobilka TS, Choi HJ, Kuhn P, Weis WI, Kobilka BK, et al. (2007) High-resolution crystal structure of an engineered human beta2-adrenergic G protein-coupled receptor. *Science* **318:**1258–1265.

Conn PM, Ulloa-Aguirre A, Ito J, and Janovick JA (2007) G protein-coupled receptor trafficking in health and disease: lessons learned to prepare for therapeutic mutant rescue in vivo. *Pharmacol Rev* **59:**225–250.

Dong C, Filipeanu CM, Duvernay MT, and Wu G (2007) Regulation of G protein-coupled receptor export trafficking. *Biochim Biophys Acta* **1768:**853–870.

Dong C and Wu G (2006) Regulation of anterograde transport of α2-adrenergic receptors by the N termini at multiple intracellular compartments. *J Biol Chem* **281:**38543–38554.

Dong C and Wu G (2007) Regulation of anterograde transport of adrenergic and angiotensin II receptors by Rab2 and Rab6 GTPases. *Cell Signal* **19:**2388–2399.

Dong C, Zhou F, Fugetta EK, Filipeanu CM, and Wu G (2008) Endoplasmic reticulum export of adrenergic and angiotensin II receptors is differentially regulated by Sar1 GTPase. *Cell Signal* **20:**1035–1043.

Duvernay MT, Zhou F, and Wu G (2004) A conserved motif for the transport of G protein-coupled receptors from the endoplasmic reticulum to the cell surface. *J Biol Chem* **279:**30741–30750.

Ferreira PA, Nakayama TA, Pak WL, and Travis GH (1996) Cyclophilin-related protein RanBP2 acts as chaperone for red/green opsin. *Nature* **383:**637–640.

Filipeanu CM, Zhou F, Claycomb WC, and Wu G (2004) Regulation of the cell surface expression and function of angiotensin II type 1 receptor by Rab1-mediated endoplasmic reticulum-to-Golgi transport in cardiac myocytes. *J Biol Chem* **279:**41077–41084.

Filipeanu CM, Zhou F, Fugetta EK, and Wu G (2006) Differential regulation of the cell-surface targeting and function of β- and α1-adrenergic receptors by Rab1 GTPase in cardiac myocytes. *Mol Pharmacol* **69:**1571–1578.

Fritze O, Filipek S, Kuksa V, Palczewski K, Hofmann KP, and Ernst OP (2003) Role of the conserved NPxxY(x)5,6F motif in the rhodopsin ground state and during activation. *Proc Natl Acad Sci U S A* **100:**2290–2295.

Heilker R, Manning-Krieg U, Zuber JF, and Spiess M (1996) In vitro binding of clathrin adaptors to sorting signals correlates with endocytosis and basolateral sorting. *EMBO J* **15:**2893–2899.

Heymann JA and Subramaniam S (1997) Expression, stability, and membrane integration of truncation mutants of bovine rhodopsin. *Proc Natl Acad Sci U S A* **94:**4966–4971.

Hunziker W and Fumey C (1994) A di-leucine motif mediates endocytosis and basolateral sorting of macrophage IgG Fc receptors in MDCK cells. *EMBO J* **13:**2963–2969.

Lu M, Echeverri F, and Moyer BD (2003) Endoplasmic reticulum retention, degradation, and aggregation of olfactory G-protein coupled receptors. *Traffic* **4:**416–433.

Ma D, Zerangue N, Lin YF, Collins A, Yu M, Jan YN, and Jan LY (2001) Role of ER export signals in controlling surface potassium channel numbers. *Science* **291:**316–319.

McLatchie LM, Fraser NJ, Main MJ, Wise A, Brown J, Thompson N, Solari R, Lee MG, and Foord SM (1998) RAMPs regulate the transport and ligand specificity of the calcitonin-receptor-like receptor. *Nature* **393:**333–339.

Mizrachi D and Segaloff DL (2004) Intracellularly located misfolded glycoprotein hormone receptors associate with different chaperone proteins than their cognate wild-type receptors. *Mol Endocrinol* **18:**1768–1777.

Morello JP and Bichet DG (2001) Nephrogenic diabetes insipidus. *Annu Rev Physiol* **63:**607–630.

Morello JP, Salahpour A, Petäjä-Repo UE, Laperrière A, Lonergan M, Arthus MF, Nabi IR, Bichet DG, and Bouvier M (2001) Association of calnexin with wild type and mutant AVPR2 that causes nephrogenic diabetes insipidus. *Biochemistry* **40:**6766–6775.

Nishimura N and Balch WE (1997) A di-acidic signal required for selective export from the endoplasmic reticulum. *Science* **277:**556–558.

Pankevych H, Korkhov V, Freissmuth M, and Nanoff C (2003) Truncation of the A1 adenosine receptor reveals distinct roles of the membrane-proximal carboxyl terminus in receptor folding and G protein coupling. *J Biol Chem* **278:**30283–30293.

Petaja-Repo UE, Hogue M, Laperriere A, Walker P, and Bouvier M (2000) Export from the endoplasmic reticulum represents the limiting step in the maturation and cell surface expression of the human delta opioid receptor. *J Biol Chem* **275:**13727–13736.

Pierce KL, Premont RT, and Lefkowitz RJ (2002) Seven-transmembrane receptors. *Nat Rev Mol Cell Biol* **3:**639–650.

Robben JH, Sze M, Knoers NV, and Deen PM (2006) Rescue of vasopressin V2 receptor mutants by chemical chaperones: specificity and mechanism. *Mol Biol Cell* **17:**379–386.

Robert J, Auzan C, Ventura MA, and Clauser E (2005) Mechanisms of cell-surface rerouting of an endoplasmic reticulum-retained mutant of the vasopressin V1b/V3 receptor by a pharmacological chaperone. *J Biol Chem* **280:**42198–42206.

Rosenbaum DM, Cherezov V, Hanson MA, Rasmussen SG, Thian FS, Kobilka TS, Choi HJ, Yao XJ, Weis WI, Stevens RC, et al. (2007) GPCR engineering yields high-resolution structural insights into beta2-adrenergic receptor function. *Science* **318:**1266–1273.

Schülein R, Hermosilla R, Oksche A, Dehe M, Wiesner B, Krause G, and Rosenthal W (1998) A dileucine sequence and an upstream glutamate residue in the intracellular carboxyl terminus of the vasopressin V2 receptor are essential for cell surface transport in COS.M6 cells. *Mol Pharmacol* **54:**525–535.

Tan CM, Brady AE, Nickols HH, Wang Q, and Limbird LE (2004) Membrane trafficking of G protein-coupled receptors. *Annu Rev Pharmacol Toxicol* **44:**559–609.

Ulloa-Aguirre A, Janovick JA, Brothers SP, and Conn PM (2004) Pharmacologic rescue of conformationally-defective proteins: implications for the treatment of human disease. *Traffic* **5:**821–837.

von Zastrow M (2003) Mechanisms regulating membrane trafficking of G protein-coupled receptors in the endocytic pathway. *Life Sci* **74:**217–224.

Wang X, Matteson J, An Y, Moyer B, Yoo JS, Bannykh S, Wilson IA, Riordan JR, and Balch WE (2004) COPII-dependent export of cystic fibrosis transmembrane conductance regulator from the ER uses a di-acidic exit code. *J Cell Biol* **167:**65–74.

Wu G, Zhao G, and He Y (2003) Distinct pathways for the trafficking of angiotensin II and adrenergic receptors from the endoplasmic reticulum to the cell surface: Rab1-independent transport of a G protein-coupled receptor. *J Biol Chem* **278:**47062–47069.

Zhou F, Filipeanu CM, Duvernay MT, and Wu G (2006) Cell-surface targeting of alpha2-adrenergic receptors—inhibition by a transport deficient mutant through dimerization. *Cell Signal* **18:**318–327.

Address correspondence to: Dr. Guangyu Wu, Department of Pharmacology and Experimental Therapeutics, Louisiana State University Health Sciences Center, 1901 Perdido Street, New Orleans, LA 70112. E-mail: gwu@lsuhsc.edu